

OBSERVATION OF NANO SIZED PARTICLES IN PROTON IRRADIATED PM-355 POLYMER WITH X-RAY DIFFRACTION (XRD) AND MORPHOLOGICAL STUDIES

S. MANSOOR ALI^{a*}, A. KAYANI^b, M. S. AL GARAWI^a,
S. S. AL-GHAMDI^a, S. A. AL-SALMAN^a, M. R. BAIG^{a*}, T. S. ALKHURAJI^c.

^a*Department of Physics and Astronomy, College of Science, P.O BOX 2455, King Saud university Riyadh Saudi Arabia*

^b*Department of Physics, Western Michigan University, Kalamazoo, MI 49008, USA*

^c*National Center for Irradiation Technology, King Abdulaziz City for Science & Technology*

The samples were irradiated by 5 MeV protons with fluence of 1.0×10^{13} ions/cm², 5.0×10^{13} ions/cm², 1.0×10^{14} ions/cm², 5.0×10^{14} ions/cm² and 1.0×10^{15} ions/cm². A non-irradiated reference sample as well as irradiated samples were subjected to X-ray diffraction (XRD), Field effect scanning electron microscopy (FESEM), and Fourier transform infrared (FTIR) spectroscopy. The XRD study indicates the gradual increase in the intensity of the X-ray scattering with increasing proton ion fluence. The crystallinity, micro strain, dislocation density and distortion parameters were found to be increasing with fluence whereas the crystalline size(L) decreases to nano-sized particles at the high proton fluences as compared to the reference. The generation of nanoparticles on the surface at the highest proton fluence have been further confirmed by FESEM morphology. It is believed that generation of nano particles on surface with Proton irradiation might be due to chain scission process. FTIR spectra also show changes in intensity of the typical bands after irradiation. The results obtained from the present investigation can be used successfully in heavy ion dosimetry using well known techniques.

(Received April 20, 2017; Accepted July 26, 2017)

Keywords: Proton irradiation, Crystallinity, Nano particle generation, Morphology, Field effect Scanning electron microscopy

1. Introduction

Studies of ion beam effects on polymeric solid state nuclear track detectors (SSNTDs) have gained significance in recent years. This is because of potential applications of SSNTDs in biological filters, in detection of light ions, radiation dosimetry for use in ion track etching, magneto resistive sensors and Electromagnetic interference (EMI) shielding [1–6].

The radiation processing can play a pivotal role in the drastic modification of materials. Ionizing irradiation deposits energy in the material and causes irreversible changes in the macromolecular structure of the SSNTDs. The most prominent effects of radiation on polymers involve a change of phase in the absorbing material due to chain scission, radical composition, bond breaking, the creation of unsaturated bonds, intermolecular cross-linking, free radical formation, hydrogen release and some oxidation reactions [7, 8]. All of these changes introduce defects inside the polymeric material which are responsible for changes in the optical, structural, thermal and electrical properties of the polymers [9].

The SSNTDs CR-39, PM-355 and PM-500 all have the same chemical composition: C₁₂H₁₈O₇ (polycarbonate of allyl diglycol), but have differences in the plasticizing additives, curing cycles, extrusion and quenching processes [10]. The polymer PM-355 is the best one,

*Corresponding author: mrehaig@ksu.edu.sa

mainly for the detection of light ions including protons, deuterons, He, C, and S ions. Therefore, this detector was mostly used in the plasma experiments [11-14] and was also recommended as a suitable analytical tool for the laser-plasma experiments [15].

From the above discussion and to the best of our knowledge, very few attempts have been carried out on PM-355 SSNTDs to study their electrical, thermal, chemical and structural properties as a function of proton fluence [16, 18]. Radiation-induced modifications for many other polymeric nuclear track detectors (viz. CR-39, Makrofol KG, PET, etc.), have been studied extensively, as the optical, chemical, structural, and thermal properties may be greatly affected by radiation [19–22]. In the present investigation, the effects of proton irradiation on the generation of nano particles in this material irradiated with higher doses of proton fluences, have been considered in order to improve their performance for diverse industrial applications.

2. Experimental details

Ion beam irradiations of PM-355 samples were carried out using the 6 MV Van de Graff accelerator at the University of Western Michigan. Small circular sections of roughly 0.5 cm² in area was exposed to 5 MeV protons with fluence of 1.0×10^{13} ions/cm², 5.0×10^{13} ions/cm², 1.0×10^{14} ions/cm², 5.0×10^{14} ions/cm² or 1.0×10^{15} ions/cm² respectively. The ion beam was allowed to pass through a gold foil to diverge the beam, followed by an 8 mm diameter circular collimator, which defines the area of the sample exposed to the ion beam. Prior to the beam irradiation, an image of the beam on the sample was obtained using photographic film. As a precautionary measure the samples were kept in the irradiation chamber at $\sim 10^{-6}$ Torr to reduce the activity if any, however no such indications has been noticed after 24 hours as checked by the G.M counter. All samples including the reference were covered in a tissue paper and then wrapped with large number of turns of aluminum foil and then put in the shielding box. XRD, Field Effect Scanning electron Microscopy (FESEM) and Fourier Transform Infrared(FTIR) Spectroscopy on samples were performed in the laboratories of King Saud University (Saudi Arabia).

3. Results and discussion

To study the effect of proton irradiation of PM-355 SSNTDs, X-ray diffraction measurements were carried out on the samples in the angular range 16–32°. X-ray diffraction(XRD) patterns were taken with Analytical X³pert instrument equipped with a Cu tube source with X-ray wavelength of 1.5406 Å. Kumar et.al (2012) have clearly reported in their published work that the pristine sample of PM-355 is partly crystalline[7]. Al-Salhi.et.at (2017) very recently has reported that the reference sample of PM-355 is partially crystalline with dominant amorphous phase [24]. The X-ray diffraction patterns of the non-irradiated reference sample and the irradiated PM-355 polymers are shown in Fig. 1. It is observed, that the polymer is partly crystalline with a dominant amorphous phase. The diffraction pattern of the non-irradiated PM-355 shows a broad peak at 20.52° which is characteristic of an amorphous structure. While for the irradiated samples the peak intensity increases, this demonstrates that the crystalline structure has been increased as a result of proton irradiatio . Ivan et.al.(2007) has reported that ions irradiation induced crystallization in amorphous selenium films[25]. The observed changes in the X-ray diffraction pattern are thought to be due to the disordering of the original structure of PM-355 due to irradiation [26].

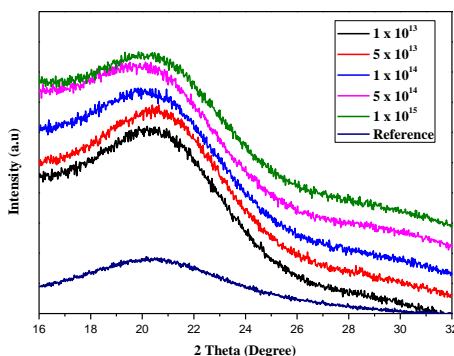


Fig. 1. XRD spectra of PM-355 SSNTDs with and without proton irradiation

The percentage of crystallinity X_c % is measured as a ratio of crystalline area to total area and is given by [27]

$$X_c \% = \left\{ \frac{A_c}{A_a + A_c} \right\} \times 100\% \quad (1)$$

Where A_c is the area of the crystalline phase, A_a is the area of the amorphous phase and X_c is the percentage crystallinity. The value of X_c has been calculated using Eq. 1 and given in table 1. It is noticed that the crystallinity percentage increases in PM-355 as the proton radiation fluence is increased.

Moreover, the crystallite size (L), inter chain distance (r), inter planar distance (d), micro strain (ε), dislocation density (δ) and distortion parameters (g) were calculated as follows [28-32]:

$$L = \frac{\lambda}{b \cos \theta} \quad (2)$$

$$r = \frac{5}{8} \frac{\lambda}{\sin \theta} \quad (3)$$

$$d = \frac{\lambda}{2 \sin \theta} \quad (4)$$

$$\varepsilon = \frac{b \cos \theta}{4} \quad (5)$$

$$\delta = \frac{1}{L^2} \quad (6)$$

$$g = \frac{b}{\tan \theta} \quad (7)$$

where $\lambda = 0.154$ nm is the wavelength of the Cu $K\alpha$ X-ray radiation used, b is the full width at half maximum of the diffraction peak (in radians) and θ is the Bragg angle. The structural parameters above were calculated from the XRD peak of the non-irradiated reference and the irradiated PM-355 and are shown in table 1. It can be seen that the crystallite size decreases considerably as the proton radiation fluence increases. In the reference sample size of 167 nm decreases to 86.4 nm as a result of 1×10^{15} proton fluence. Inter chain and inter planar distances were only slightly changed because the angle of the peak did not vary significantly as a result of irradiation. The micro strain, distortion parameters and dislocation density increases with an increase in the proton radiation fluence. This is due to the mismatching of the atoms or ions. It is clear from the table that the structural parameters (ε , δ , g) increase with an increase in the proton fluence.

Table 1. Structural parameters of reference and proton irradiated PM-355 SSNTDs

Fluence (ions/cm ²)	X_c (%)	L (Å)	r (Å)	d (Å)	ϵ	δ ($\times 10^{17}$)	g (%)
0	58	16.76	5.21	4.35	3.11	3.56	36.89
1×10^{13}	65	9.73	5.17	4.28	3.36	10.56	41.52
5×10^{13}	66	9.56	5.13	4.25	3.41	10.94	46.86
1×10^{14}	68	9.17	5.24	4.45	3.79	11.89	49.73
5×10^{14}	71	8.95	5.27	4.50	4.21	12.48	52.38
1×10^{15}	73	8.64	5.23	4.28	4.31	13.4	57.21

The effect of proton irradiation on the physical and chemical changes in the polymeric PM-355 SSNTD was also investigated by FTIR spectroscopy. The influences of radiation are predictable from the relative increase or decrease in the transmittance intensity of the characteristic bands related to the functional groups present in the polymers [33]. The FTIR spectra were obtained in the wavenumber range 600–4000 cm⁻¹, for the non-irradiated reference and irradiated samples. The typical peaks of PM-355 are observed at 1235, 1735 and 2917 cm⁻¹ corresponding to the C–O–C bond, C=O bond and C–H bond, respectively. Figure 2 shows the FTIR spectra of the reference and the proton irradiated PM-355 at different proton radiation fluence. It has been observed that the decrease in peak intensity of the C=O, C–O–C and C–H bands after irradiation and with increasing radiation fluence (as shown in Fig.2) is associated with the cleavage of the carbonate linkage and to the –H abstraction from the back bone of the polymer, associated with the formation of CO₂ and –OH with varying concentrations.

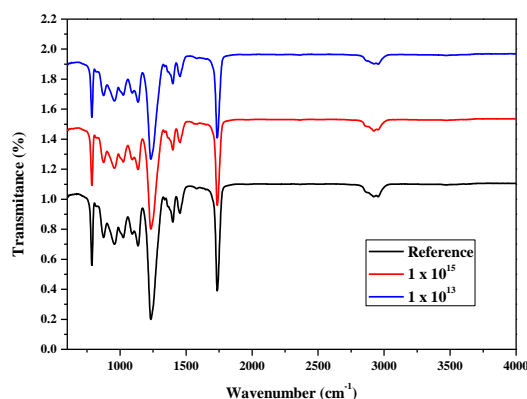


Fig. 2. FTIR spectra of reference and proton irradiated PM-355 SSNTDs

Structural and surface morphology of the irradiated and reference samples were studied with FESEM micrographs. FESEM micrographs were taken with JSM-6380 LA machine from JEOL. It has resolution 3.0 NM (30 kV, WD 8 mm, SEI). Figure 3 shows FESEM micrographs of the surfaces of the non-irradiated reference and proton irradiated PM-355 SSNTDs. In Figure 3(a) for the non-irradiated reference, a large area of surface is relatively smooth and homogenous when compared to the irradiated samples. Figure 3(b) shows nonhomogeneous surfaces with a continuous matrix which becomes rough at low proton radiation fluence. The FESEM micrographs of irradiated PM-355 SSNTDs reveal the formation of little cavities with an interpenetrating network as shown in Figure 3(c). In Figure 3(d) it can be seen that the higher radiation fluence improves the homogeneity of the surface with the generation of nanoparticles of average size about 88 nm. This may be due to oxidative degradation. These findings indicate that the improvement in compatibility is greater in case of proton irradiation.

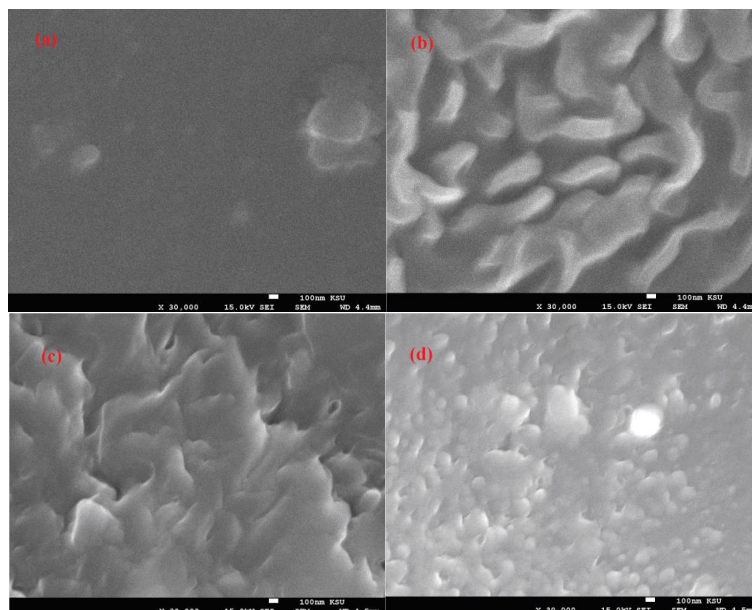


Fig. 3. FESEM morphology of (a) reference, (b) 1×10^{13} , (c) 1×10^{14} and (d) 1×10^{15} ions/cm² proton irradiated PM-355 SSNTDs

4. Conclusions

From the results we have reported and discussed for the proton ion irradiation of PM-355 polymeric solid state nuclear detectors, our conclusions can be summarized as follows. From the analysis of XRD spectra; it has been observed that there is an increase in the crystallinity and a decrease in crystallite size(L) in the nano range as a function of proton ion fluence. The calculation from XRD patterns using Scherrer equation reveal that tiny particles are generated at the surface with proton irradiation and with further increasing fluence, the sizes become smaller and smaller ultimately end up in nanosized particles which is confirmed by FESEM micrographs. The FESEM morphology shows the generation of nanoparticles on the surface at highest proton fluence studied. This is associated with the formation of free radicals as a result of the proton irradiation. FTIR spectra also show a significant change in the intensity of the typical bands after irradiation.

Acknowledgment

The authors would like to extend their sincere appreciation to the Deanship of Scientific Research at King Saud University for its funding of this research through the Research Group Project No. RGP -1436-019.

References

- [1] S.A. Durrani, Nucl. Tracks Radiat. Meas. **6**, 209 (1982).
- [2] E. Skladnik-Sadowska, J. Baranowski, M. Sadowski, Radiat. Prot. Dosim. **101**, 585 (2002).
- [3] P.P. Buford, Radiat. Meas. **40**, 146 (2005).
- [4] S.K. Chakarvarti, Radiat. Meas. **44**, 1082 (2009).
- [5] B. Adhikari, S. Majumdar, Polymers in sensor applications. Prog. Polym. Sci. **29**, 699 (2004).
- [6] J.M.G. Laranjeira, H.J.K. Azevedo, Vasconcelos de, E.A., Silva Jr., E.F. Da, Mater. Charact. **50**, 127 (2003).

- [7] V. Kumar, R.G. Sonkawade, A.S. Dhaliwal, Nuclear Instruments and Methods in Physics Research B **290**, 59 (2012).
- [8] A. Tayel, M.F. Zaki, A.B. El Basaty, Tarek M. Hegazy, Journal of Advanced Research **6**, 219 (2015).
- [9] M. Nasef, M. Dahlan, M. Khairal, Nucl. Instrum. Methods Phys. Res., Sect. B **201**, 604 (2003).
- [10] S. A. Durrani, R. K. Bull, "Solid State Nuclear Track Detection. Principles, Methods and Applications," Pergamon Press, Oxford, 1987.
- [11] A. Szydłowski, Radiation Measurements **36**(1-6), 35 (2003).
- [12] B. Sartowska, A. Szydłowski, M. Jaskola, A. Korman, Radiat. Meas. **40**, 347 (2005).
- [13] E. Składnik-Sadowska, K. Malinowski, SM.J. Adowski, K. Czaus, Radiat. Meas. **44**, 870 (2009).
- [14] A. Szydłowski, B. Sartowska, M. Jaskola, A. Korman, A. Malinowska, J. Choinski, Radiat. Meas. **44**, 798 (2009).
- [15] A. Szydłowski, J. Badziak, J. Fuchs, M. Kubkowska, P. Parys, M. Rosinski, R. Suchanska, J. Wolowski, P. Antici, A. Mancic, Radiation Measurements **44**(9-10), 881 (2009).
- [16] S.A. Nouh, A.A. Naby, H.M. El Hussien, Appl. Radiat. Isot. **65**, 1173 (2007).
- [17] S.A. Nouh, S. Bahammam, Radiat. Eff. 1 (2011).
- [18] S. Nouh, Radiat. Meas. **38**, 167 (2004).
- [19] S. Singh, S. Prasher, Radiat. Meas. **40**, 50 (2005).
- [20] P.C. Kalsi, C. Agarwal, J. Mater. Sci. **43**, 2865 (2008).
- [21] V. Kumar, R.G. Sonkawade, S.K. Chakarvarti, P. Kulriya, K. Kant, N.L. Singh, A.S. Dhaliwal, Vacuum **86**, 275 (2011).
- [22] Siddhartha, S. Aarya, K. Dev, S.K. Raghuvanshi, J.B.M. Krishna, M.A. Wahab, Radiat. Phys. Chem. **81**, 458 (2012).
- [23] M S .Alsalihi, M.R .Baig, K. Alfaramawi, M.G Alrasheedi, Radiat. Phys. Chem. **130**, 451 (2017).
- [24] I. Ivan, S. Kokenyesis, A. Csik, Chalcogenide Letters **4**(10), 115 (2007).
- [25] R.C. Ramola, Chandra, S., Negi, A., Rana, J. M. S., Annapoorni, S., Sonkawade, R. G., Kulriya, P. K., Srivastava, A., Physica B **404**, 26 (2009).
- [26] R.C. Ramola, Chandra,S., Rana, J. M. S., Sonkawade, R. G., Kulriya, P. K., Singh, F., Avasthi, D. K., Annapoorni, S., J. Phys. D: Appl. Phys. **41**, 115411 (2008b).
- [28] V. Kumar, Y. Ali, R.G. Sonkawade, A.S. Dhaliwal, Nucl. Instr. Meth B **287**, 10 (2012).
- [29] R.C. Ramola, A. Negi, A. Semwal, S. Chandra, J.M.S. Rana, R.G. Sonkawade, D. Kanjilal, J. Appl. Polym. Sci. **121**, 3014 (2011).
- [30] M. Madani, Curr. Appl. Phys. **11**, 70 (2011).
- [31] B. Mallick, T. Patel, R.C. Behera, S.N. Sarangi, S.N. Sahu, R.K. Choudhary, Nucl. Instr. Meth. B **248**, 305 (2006).
- [32] A. Vij, A.K. Chawla, R. Kumar, S.P. Lochab, R. Chandra, N. Singh, Phys. B **405**, 2573 (2010).
- [33] Kilarkaje S., Manjunatha V., Raghu S., Ambika Prasad M.V.N., and Devendrappa H., J. Phys. D: Appl. Phys. **44**, 105403 (2011).